Journal of the Korean Nuclear Society
Volume 31, Number 6, pp.572~585, December 1999

Development of a Linear Stability Analysis Model for Vertical Boiling Channels Connecting with Unheated Risers

Dae-Hyun Hwang, Yeon-Jong Yoo, and Seong-Quun Zee
Korea Atomic Energy Research Institute
150 Dukjin-dong, Yusong-gu, Taejon 305-353, Korea
dhhwang@kaeri.re.kr

(Received June 9, 1999)

Abstract

The characteristics of two-phase flow instability in a vertical boiling channel connecting with an unheated riser are investigated through the linear stability analysis model. Various two-phase flow models, including thermal non-equilibrium effects, are taken into account for establishing a physical model in the time domain. A classical approach to the frequency response method is adopted for the stability analysis by employing the D-partition method. The adequacy of the linear model is verified by evaluating experimental data at high quality conditions. It reveals that the flow-pattern-dependent drift velocity model enhances the prediction accuracy while the homogeneous equilibrium model shows the most conservative predictions. The characteristics of density wave oscillations under low-power and low-quality conditions are investigated by devising a simple model which accounts for the gravitational and frictional pressure losses along the channel. The necessary conditions for the occurrences of type-I instability and flow excursion are deduced from the one-dimensional D-partition analysis. The parametric effects of some design variables on low quality oscillations are also investigated.

Key Words : density wave oscillation, type-I instability, D-partition method, flow excursion

1. Introduction

As recognized in BWR design, the two-phase flow instability is an important design parameter for the parallel-channel type reactor core since it may result in an abrupt change or oscillation of operating conditions which will cause local burnout. In most cases, the two-phase flow instability is highly concerned in association with bulk boiling systems. However, even though the bulk fluid at the core exit region maintains at a subcooled condition, local boiling can occur at the exit of the hottest fuel assembly. Parallel channel instabilities may occur when a small number of heated boiling channels are hydraulically operated in parallel with many non-boiling channels. An example of this kind of core configuration can be found in the pressure-tube-type reactor[1]. If the total flow through all channels is maintained at a constant value, considerable flow changes can

occur in the boiling channel with only minor flow changes in the non-boiling channels. In this case, the boiling channel is essentially operating with constant imposed pressure drop, and can either exhibit flow excursions or density wave oscillations. It is known that density wave oscillations are due to multiple regenerative feedback amongst the flow rate, the vapor generation rate, and the pressure drop along the channel. If a small fluctuation is exerted on the inlet velocity of a boiling channel, it may create an enthalpy perturbation in the single-phase region. When this perturbation reaches the boiling boundary, it is transformed into a two-phase mixture density perturbation, which travels the channel with kinematic wave velocity, and results in a dynamic pressure drop fluctuation in the two-phase region. If the total pressure drop remains constant along the channel, this two-phase pressure drop fluctuation produces an opposite perturbation of a single-phase pressure drop, which in turn creates a feedback perturbation of inlet velocity. Since the kinematic wave velocity is finite, there is a phase-shift between the exerted fluctuation and the feedback perturbation of inlet velocity, and under certain circumstances may result in self-excited oscillation.

A lot of studies have been devoted to this area during the last several decades, and as a result, many of the phenomenological questions are presently resolved[2,3]. On density wave oscillations, a systematic study was conducted by Fukuda & Kobori[4], and they identified two typical types of the oscillations. The 'type-I' instability was found to be governed by gravitational pressure drop under the conditions of low exit quality, while the 'type-II' instability was dominated by the frictional pressure drop of the two-phase flow at high exit qualities. For a vertical boiling channel with an unheated riser, both types of instabilities may occur depending on the operating conditions. In this study we adopted Saha' s thermal non-equilibrium model[5] as a reference for establishing a linear stability analysis model. Saha' s model is an extended version of Ishii' s drift flux model[6] by accounting for the subcooled boiling effects. He conducted a set of experiments in the freon test loop to investigate density wave oscillation under high quality conditions. We extended Saha' s non-equilibrium model to the boiling channel connecting with unheated riser. Furthermore, various formulations of the two-phase flow velocity and temperature are examined. In the aspect of reactor safety, type-I oscillation is highly undesirable since it may cause local burnout under low-power and low-quality conditions. Recently, experimental and analytical studies have been performed on low-power and low-quality oscillations in a two-phase natural circulation loop related to the design of advanced boiling water reactors[7,8]. Although the knowledge on the basic phenomena related to the type-I instability is well established, the equations describing the system dynamics are very complex and as the result, it is hard to clearly understand the parametric influence on the low quality oscillations. The purposes of this study are, firstly, to develop a linear stability analysis model applicable to an advanced reactor core which consists of parallel-channel type fuel assemblies, and secondly, to provide a basic understanding on low quality oscillations by developing a simple linear model.

2. Establishment of a Linear Model

2.1. Physical Model in the Time-domain

The schematic diagram of the boiling channel considered in this study is shown in Fig. 1. It consists of the unheated inlet section, heated section, and unheated riser section. The heated

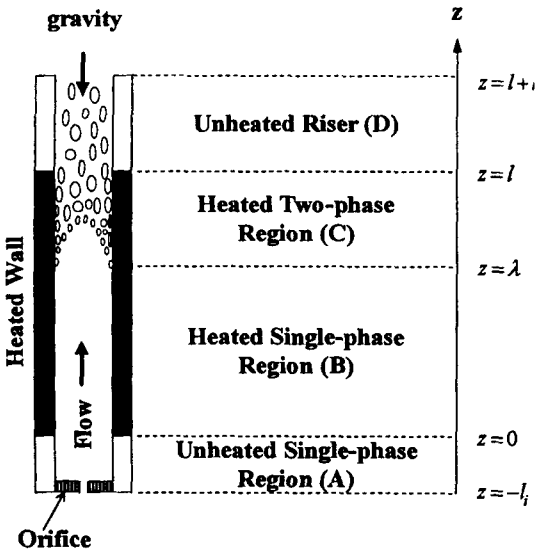

Fig. 1. Schematic Diagram of a Vertical Boiling Channel

section is divided into the single-phase and two-phase regions. The length of the heated section is l and significant vapor generation starts at a distance λ from the inlet of the heated region. The following assumptions are made in the analysis:

(a) Constant thermodynamic properties are used in a given system pressure.

(b) Axial heat flux distribution is uniform.

(c) The drift flux model is used to formulate the problem in the two-phase mixture region.

(d) Thermal non-equilibrium effects are taken into account through a subcooled boiling model.

(e) Inlet velocity perturbation is considered.

According to the assumption (a), the momentum conservation equations can be decoupled from the mass and energy conservation equations. The mass and energy conservation equations in the heated two-phase mixture region can be transformed into the volumetric flux equation and the density propagation equation[9] which are expressed as,

$$\frac{\partial j}{\partial z}=\Omega, \tag{1}$$

and

$$\frac{\partial \rho_m}{\partial t}+C_k\frac{\partial \rho_m}{\partial z}=-\rho_m\Omega, \tag{2}$$

respectively. The one dimensional momentum conservation equation in this region becomes

$$\frac{\partial v_m}{\partial t}+v_m\frac{\partial v_m}{\partial z}=-\frac{1}{\rho_m}\frac{\partial P}{\partial z}-\frac{f_m}{2D}v_m^2-g-\frac{1}{\rho_m}\frac{\partial}{\partial z}\left\{\frac{\rho_f\rho_g}{\rho_m}\frac{\alpha}{1-\alpha}V_{gj}^2\right\}, \tag{3}$$

where V_{gj} is the drift velocity averaged over the cross-sectional area of the channel. As noted by Zuber[10], the perturbations of the mixture density are propagated through the two-phase mixture with the velocity of kinematic waves. The kinematic wave velocity(C_k) and the superficial velocity(j) are related to the center-of-mass velocity of the mixture (v_m) as follows.

$$C_k=j+V_{gj}+\alpha\frac{\partial V_{gj}}{\partial \alpha}, \tag{4}$$

$$j=v_m+\alpha\frac{(\rho_L-\rho_g)}{\rho_m}V_{gj}. \tag{5}$$

The mixture density is expressed as

$$\rho_m=\alpha\rho_g+(1-\alpha)\rho_L \tag{6}$$

The vapor generation rate for the thermal non-equilibrium conditions is obtained from the Zuber model[11] which is expressed as

$$\Gamma_g(z)=\Gamma_{g,eq}\left[1-\exp\left(-\frac{z-\lambda}{\Delta l}\right)\right], \tag{7}$$

where the vapor generation rate at the thermal equilibrium condition is

$$\Gamma_{g,eq}=\frac{q''\xi_h}{Ah_{fg}}, \tag{8}$$

and

$$\Delta l=\frac{GA\Delta h_\lambda}{q''\xi_h} \tag{9}$$

The local subcooling at the OSV(Onset of Significant Void) condition was calculated from the Saha-Zuber model[12] which is given as,

$$\Delta h_{\lambda} \equiv h_f - h_{\lambda} = 0.0022 \frac{q'' \cdot D_{hy} \cdot c_{pf}}{k_f}, \quad \text{for } P_e \le 70{,}000, \quad (10)$$

$$\Delta h_{\lambda} = 154 \frac{q''}{G}, \quad \text{for } P_e > 70{,}000. \quad (11)$$

In order to close the system of equations, we introduced appropriate models for the friction loss coefficient (f_m) and the drift velocity (V_{gj}) as well as the equation of state. The single-phase friction loss coefficient of the boiling channel is calculated by[13]

$$f = 27.6 \cdot \mathrm{Re}^{-0.76}, \text{ for } \mathrm{Re} < 4070, \quad (12)$$

$$f = 0.49 \cdot \mathrm{Re}^{-0.275}, \text{ otherwise.} \quad (13)$$

The drift velocity of the vapor is calculated from Ishii' s flow-pattern-dependent model[14] which is given as,

$$V_{gj} = \min\left(V_{gj,1}, V_{gj,2}\right), \quad (14)$$

where

$$V_{gj,1} = (C_0 - 1) \cdot j + \sqrt{2}\left[\frac{\sigma g \Delta\rho}{\rho_f^2}\right]^{0.25}, \quad (15)$$

for bubbly-churn flow regime,

and

$$V_{gj,2} = \frac{1-\alpha}{\alpha + \sqrt{\dfrac{1+75(1-\alpha)}{\sqrt{\alpha}} \dfrac{\rho_g}{\rho_f}}} \cdot \left[j + \sqrt{\frac{\Delta\rho \cdot g \cdot D \cdot (1-\alpha)}{0.015 \cdot \rho_f}} \right], \quad (16)$$

for annular flow regime.

In the bubbly-churn flow region, the distribution parameter is calculated by

$$C_0 = 1.2 - 0.2\sqrt{\frac{\rho_g}{\rho_f}}. \quad (17)$$

2.2. Linearized Model in the Frequency-domain

In order to apply the frequency response method, we first linearize the governing equations using the first-order perturbation technique. The linearized time-domain differential equations are converted to an equivalent set of frequency-domain algebraic equations through the Laplace transformation. The dynamic response of the system with respect to the inlet velocity perturbation can be represented by integrating the perturbed momentum equation. For the heated two-phase region the pressure drop is expressed as

$$\Delta P_C = \int_{\lambda(t)}^{l} \left[\rho_m \left\{ \frac{\partial v_m}{\partial t} + v_m \frac{\partial v_m}{\partial z} + g + \frac{f_m}{2D} \cdot v_m^2 \right\} + \frac{\partial}{\partial z} \left\{ \frac{\rho_L \rho_g}{\rho_m} \frac{\alpha}{(1-\alpha)} V_{gj}^2 \right\} \right] \cdot dz, \quad (18)$$

where, $\lambda = \bar{\lambda} + \delta\lambda$, $v_m = \bar{v}_m + \delta v_m$ and $\rho_m = \bar{\rho}_m + \delta\rho_m$. Important kinematic variables dominating the dynamic response are the boiling boundary, the mixture density, and the mixture velocity. In the liquid phase, assuming that the liquid velocity is independent of the flow enthalpy, the following relationship is valid.

$$\int_0^{\lambda(t)} dz = \int_{\tau_1}^{\tau_2} v(t) dt \quad (19)$$

According to the frequency response method, the inlet velocity perturbation is expressed as

$$v(t) = \bar{v}_i + \varepsilon e^{st}, \quad (20)$$

where s is a complex variable. Since $\lambda(t) = \bar{\lambda} + \delta\lambda(t)$, we can obtain the perturbation of the boiling boundary as

$$\delta\lambda(t) = \Lambda_1(s) \cdot \delta v, \quad (21)$$

where

$$\Lambda_1(s) = \frac{1 - e^{-s\tau_{12}}}{s} \quad (22)$$

The residence time in the heated single-phase region can be calculated from the energy balance equation. That yields

$$\bar{\tau}_{12} \equiv \tau_2 - \tau_1 = \frac{\rho_f \cdot A}{q'' \cdot \xi_h} \cdot (\Delta h_{sub} - \Delta h_\lambda) \quad (23)$$

The local subcooling at the OSV location, Δh_λ, becomes zero for the thermal equilibrium condition.

The perturbation of the mixture density in the two-phase heated region is calculated from the density propagation equation and the perturbation of the kinematic wave velocity which can be obtained from the volumetric flux equation. By integrating the volumetric flux equation for the heated two-phase region, we can obtain

$$\delta C_k(z,t) = \Lambda_3(z,s) \cdot \delta v \quad (24)$$

where

$$\Lambda_3(z,s) = 1 - \bar{\Omega} \cdot \Lambda_1(s) + \int_{\bar{\lambda}}^{z} \frac{\delta\Omega}{\delta v} dz \quad (25)$$

For thermal equilibrium condition,

$$\Lambda_3(s) = 1 - \Omega_{eq} \cdot \Lambda_1(s) \quad (26)$$

where

$$\Omega_{eq} = \frac{\Delta\rho}{\rho_f \rho_g} \cdot \frac{q'' \xi_h}{A h_{fg}} \quad (27)$$

The density propagation equation is linearized by introducing the previous study[5]. After long manipulation, the perturbation of the mixture density in the heated two-phase region can be expressed as [9]

$$\frac{\delta\rho_m(z,t)}{\rho_f} = \Lambda_4(z,s) \cdot \delta v \quad (28)$$

For thermal equilibrium condition,

$$\Lambda_4(z,s) = \left(\frac{C_z}{C_\lambda}\right)^{-\frac{s}{\Omega_{eq}}-1} \left(\frac{\Omega_{eq}}{C_\lambda}\right) \cdot \left[\Lambda_1(s) + \frac{\Lambda_3(s)}{s - \Omega_{eq}} \left\{ \left(\frac{C_z}{C_\lambda}\right)^{\frac{s}{\Omega_{eq}}-1} - 1 \right\}\right] \quad (29)$$

where

$$C_z = \bar{v}_i + V_{gj} + \Omega_{eq}\left(z - \bar{\lambda}\right) \quad (30)$$

and

$$C_\lambda = \bar{v}_i + V_{gj} \quad (31)$$

The perturbation of the mixture velocity in the heated two-phase region is related to the perturbation of the mixture density through eqs. (4) and (5). In order to evaluate the last term on the right-hand-side of eq. (4), we consider Ishii' s *flow-pattern-dependent* drift velocity model given by eqs. (15) and (16). The drift velocity is not influenced by the void fraction at the bubbly flow region. At the annular flow region, if $\rho_g/\rho_f \ll 1$, the distribution parameter (C_0) should be close to unity and the variation of the drift velocity with respect to the void fraction can be neglected. Then we obtain the following relationship.

$$v_m(z,t) = C_k(z,t) - \frac{\rho_f V_{gj}}{\rho_m(z,t)} \quad (32)$$

Thus,

$$\delta v_m(z,t) = \Lambda_5(z,s) \cdot \delta v \quad (33)$$

where

$$\Lambda_5(z,s) = 1 - \Omega_{eq}\Lambda_1(s) + \left(\frac{C_z}{C_\lambda}\right)^2 V_{gj} \cdot \Lambda_4(z,s) \quad (34)$$

for thermal equilibrium condition.

Since it was assumed that the volumetric flux in the unheated riser region is constant, the mixture velocity in the riser section (i.e., unheated two-

Table 1. Components of Hydraulic Impedance in a Vertical Boiling Channel

	Single-phase flow: $\Gamma(s)$		Two-phase flow: $\Pi(s)$	
	Unheated (A)	Heated (B)	Heated (C)	Unheated (D)
Temporal acceleration	$sP_f l_l$	$sP_f \lambda$	$\Lambda_{C,a}(s)$	$\Lambda_{D,a}(s)$
Convective acceleration	0	0	$\Lambda_{C,c}(s)$	0
Gravitational loss	0	$gP_f \bar{\tau}_{12} H(s)$	$\Lambda_{C,g}(s)$	$\Lambda_{D,g}(s)$
Frictional loss	$\Lambda_{A,f}(s)$	$\Lambda_{B,f}(s)$	$\Lambda_{C,f}(s)$	$\Lambda_{D,f}(s)$
Drift stress	0	0	$\Lambda_{C,d}(s)$	$\Lambda_{D,d}(s)$

phase region) is independent of the axial location. Thus,

$$\frac{\delta v_{me}}{\delta v} = \left.\frac{\delta v_m}{\delta v}\right|_{z=l} \tag{35}$$

Furthermore, due to the finite kinematic wave velocity, the perturbation of the mixture density in the unheated riser region propagates with time delay from the density perturbation at the exit of the heated channel. That is,

$$\frac{\delta \rho_{me}}{\delta v} = \left.\frac{\delta \rho_m}{\delta v}\right|_{z=l} \cdot e^{-s\left(\frac{z-l}{v_{me}}\right)} \tag{36}$$

The perturbed pressure drop can be calculated by accounting for the perturbations of kinematic variables. The transfer function of the system is determined as the total pressure drop perturbation corresponding to the inlet velocity perturbation, which is frequently called the 'hydraulic impedance'. Table 1 summarizes the components of the hydraulic impedance in the vertical boiling channel, and the functional form is given in the Appendix.

The appropriate block diagram of the system is represented as shown in Fig. 2[15]. The physical meaning of the block diagram is as follows. Basically, the density wave oscillation is caused by the lag introduced into the thermal-hydraulic system due to the finite speed of propagation of the density perturbations. A perturbation in the

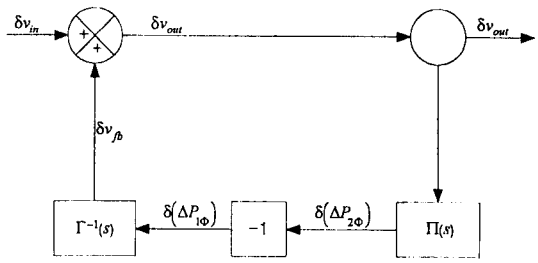

Fig. 2. Block Diagram of the Boiling System[15]

inlet velocity (δv_{in}) will create a propagating enthalpy perturbation in the single-phase region. The point where boiling begins will be perturbed by the arrival of this enthalpy wave. In the two-phase region, there will be a propagating void fraction perturbation due to the perturbation in the boiling inception point. Due to the change in flow rate and non-boiling length, there will be a perturbation in the two-phase pressure drop ($\delta(\Delta P_{2\phi}) = \Pi(s) \cdot \delta v_{out}$). Since the pressure drop across the channel is externally imposed, there must be an equal and opposite perturbation in the single phase pressure drop ($\delta(\Delta P_{1\phi}) = (-1) \cdot \delta(\Delta P_{2\phi})$). This single-phase pressure drop perturbation is equivalent to the feedback of the inlet velocity perturbation ($\delta v_{fb} = (1/\Gamma(s)) \cdot \delta(\Delta P_{1\phi})$). Because of the lags associated with the finite speed of the propagation of enthalpy and the void fraction perturbations, the feedback perturbation in the single-phase pressure drop will normally be out-of-phase with the inlet velocity perturbation.

According to this block diagram, the closed-loop transfer function of the system becomes,

$$\delta v_{out} = \frac{\Gamma(s)}{\Gamma(s)+\Pi(s)} \cdot \delta v_{in}. \quad (37)$$

Thus, the characteristic equation is,

$$\Gamma(s)+\Pi(s)=0. \quad (38)$$

2.3. Assessment of the Linear Model

The asymptotic stability of the system can be determined by the nature of the roots of the characteristic equation. The necessary condition for the asymptotic stability is that the characteristic equation has all its roots in the left-half of the s-plane. Then every component of disturbance tends to zero as time goes to infinity. Two different stability analysis methods are applied to the characteristic equation. The two-dimensional D-partition method[16] is used to obtain the stability boundary in the N_{sub}-N_{pch} plane. The stability of each D-partitioned region is checked through the Nyquist plot method[17]. If the coefficients in the characteristic equation are function of multiple system parameters, then the root-locus method can show the effect of varying only one of the parameters at a time. However, it is possible to avoid this restriction to only one system parameter by classifying the characteristic equation according to the nature of their roots instead of plotting the roots themselves, as in the root-locus method. In practice, the D-partition is made either in the one-parameter complex plane or in the two-parameter real plane. If the parameters employed are linear, the D-partition method requires a little more work and gives much more information about the stability of the system than the Nyquist criterion does.

A computer program developed in this study, ALFS[18], is applied in the analysis of experimental data of the type-II density wave oscillation. Saha[19] performed an experimental work using freon-113 as the operating fluid. The test section was a 2.743 m long, uniformly heated vertical round tube made of SS-304 with an inside diameter of 10 mm. The effects of system pressure, inlet and exit restrictions, and the inlet mass velocity were investigated by performing seven different sets of experiments. For one set of data, the system pressure, the positions of the inlet and the exit throttling valves, and the inlet mass velocity through the test section were kept constant. FLARE (Fog Loop Advanced Reactor Engineering)[20] is a high pressure steam-water loop with provision for imposing a considerable range of flow, pressure and temperature at the inlet of the test section. Flow from the loop enters an inlet reservoir from which three inlet pipes feed identical heated channels. The channels are of annular cross section, the central core being heated. The dimension of the heated section are; the heated length of 3.05 m, the heated outside diameter of 15.2 mm, and the annulus inside diameter of 19.3 mm or 20.8 mm. For each test, predetermined values of total flow, pressure and the subcooling at the channel inlet were set and maintained constant. Heater power to each of the three test sections was raised from zero by small increments until the flow trace showed pronounced oscillations.

Figures 3 and 4 show the analysis results of ALFS for these experimental data. The vertical axis of the figure indicates the predicted-to-measured power ratio at the onset of instability. Three different two-phase flow models are examined through the ALFS code: HEM (Homogeneous Equilibrium Model), DEM (Drift-flux Equilibrium Model), and DNEM (Drift-flux Non-Equilibrium Model). In view of the results so far achieved, the DNEM reveals the most accurate

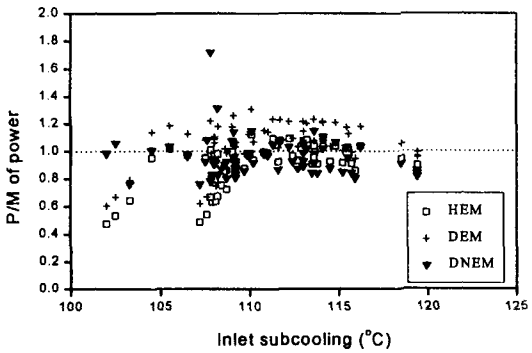

Fig. 3. Analysis of Saha' s Freon-loop Data[19] with Various Two-phase Flow Models

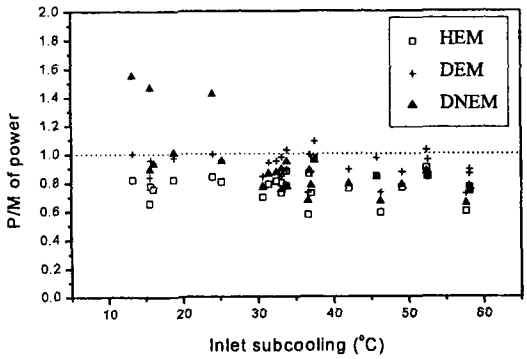

Fig. 4. Analysis of FLARE Loop Data[20] with Various Two-phase Flow Models

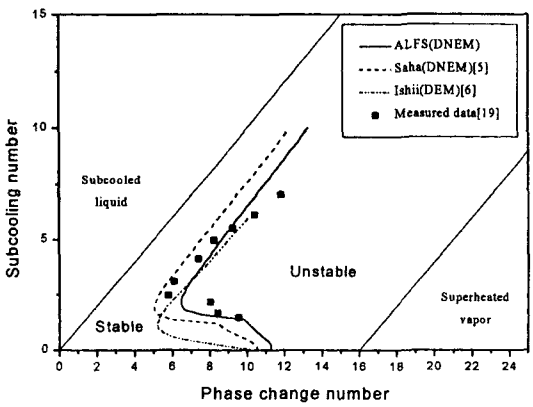

Fig. 5. Comparison with Existing Models

predictions while HEM tends to under-predict the power level triggering the density wave oscillation. For 69 data points, the mean and the standard deviation of the predicted-to-measured power at the onset of oscillation are calculated as 0.952 and 0.143, respectively, by DNEM. By employing a flow-regime-dependent model for the drift velocity[14], ALFS shows a better prediction accuracy comparing with the existing models, as shown in Fig. 5. It reveals that the Saha' s thermal non-equilibrium model predicts the system more stable at a low subcooling number, and more unstable at a high subcooling number when comparing with the Ishii' s thermal equilibrium model, as pointed out by Saha[5].

3. Development of a Simple Model for Type-I Instability

3.1. Model Development

On the basis of the linear model described in the previous sections, a simple model has been developed for the analysis of a density wave oscillation at low quality conditions by accounting for the frictional and gravitational pressure losses in the boiling channel. The frictional pressure losses at the single-phase flow region are represented by the restriction at the inlet orifice, and the effect of subcooled boiling is neglected to simplify the formulation. Assuming that the boiling length is very short under low exit quality conditions, then the transfer functions in the heated two-phase region can be approximated as,

$$\Lambda_{c,g}(s) = -g\rho_f \bar{\tau}_{12} H(s), \tag{39}$$

$$\Lambda_{c,f}(s) = -\rho_f \bar{v}_i \frac{f\bar{\lambda}}{2D} H(s). \tag{40}$$

Thus the characteristic equation of the system is obtained as

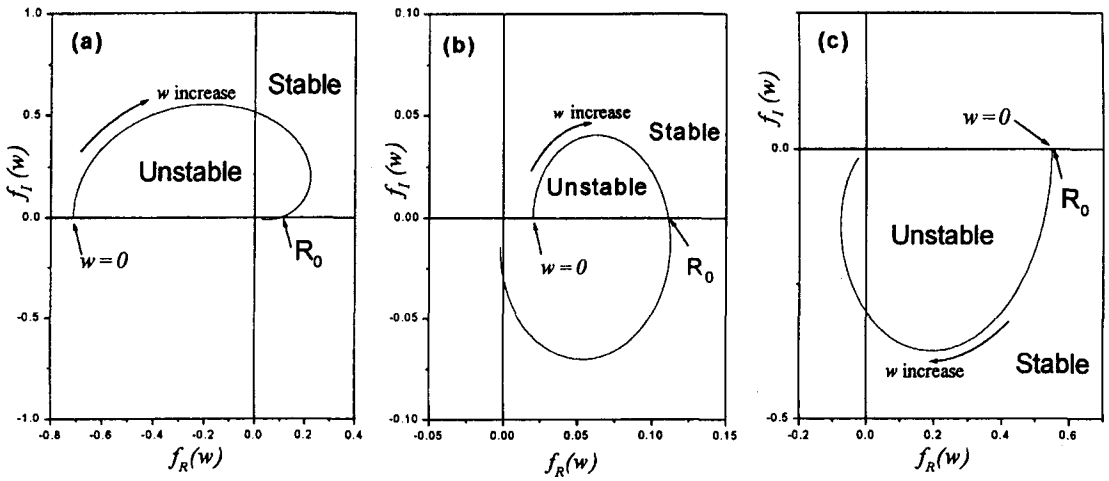

Fig. 6. D-partition Boundaries with Respect to Various K_1 Values

$$2\rho_f \bar{v}_i k_{i,eff} + \Lambda_{D,g}(s) + \Lambda_{D,f}(s) = 0 \quad (41)$$

where

$$k_{i,eff} = \frac{f_i l_i}{2D_i} + k_i + \frac{f\bar{\lambda}}{2D}. \quad (42)$$

Since the residence time in the heated two-phase mixture region is negligible, we can derive the following simplifications from eqs. (29) and (34).

$$\Lambda_4(l,s) \cong \frac{\Omega_{eq}}{C_l}\Lambda_1(s) \quad (43)$$

and

$$\Lambda_5(l,s) \cong 1 + \Omega_{eq}\left(\frac{C_r^2}{C_l}V_{gj} - 1\right)\cdot\Lambda_1(s) \quad (44)$$

where C_r=C_l/C_λ. After some manipulations, a non-dimensional characteristic equation of the system is derived as

$$\left(\frac{1-e^{-s\bar{\tau}_{12}}}{s\bar{\tau}_{12}}\right)\cdot\left(\frac{1-e^{-s\bar{\tau}_{34}}}{s\bar{\tau}_{34}}\right) - K_1\cdot\left(\frac{1-e^{-s\bar{\tau}_{12}}}{s\bar{\tau}_{12}}\right) + K_2 = 0 \quad (45)$$

where

$$K_1 = \frac{k_e + 2N_{fe}}{\frac{1}{F_r} + N_{fe}}, \quad (46)$$

and

$$K_2 = \frac{2\left(k_i + k_e + 2N_{fe}\right)\cdot\left(1+V_{gj}^*\right)}{\left(\frac{1}{F_r} + N_{fe}\right)\cdot N_{sub}} \quad (47)$$

The dimensionless parameter K_1 indicates the relative importance of the gravitational loss with respect to the frictional loss in the unheated riser region. For a gravity dominant system the Froude number decreases and results in the decrease of K_1. The dimensionless parameter K_2 also decreases for the gravity dominant system, and is inversely proportional to the subcooling number.

3.2. Model Assessment

3.2.1. Solution Method

To examine the parametric behavior of the system, we apply the one-dimensional D-partition method to the characteristic equation with respect to the parameter K_2. By substituting $s=jw$ into the characteristic equation, we can derive a pair of equations representing the real and imaginary parts of K_2. They are

$$f_R(w)=\frac{1}{\bar{\tau}_{12}\bar{\tau}_{34}w^2}\{(1-\cos w\bar{\tau}_{12})(1-\cos w\bar{\tau}_{34}) - \sin w\bar{\tau}_{12}(\sin w\bar{\tau}_{34}-w\bar{\tau}_{34}K_1)\}, \quad (48)$$

and

$$f_I(w)=\frac{1}{\bar{\tau}_{12}\bar{\tau}_{34}w^2}\{(1-\cos w\bar{\tau}_{12})(\sin w\bar{\tau}_{34} - w\bar{\tau}_{34}K_1)+\sin w\bar{\tau}_{12}(1-\cos w\bar{\tau}_{34})\}. \quad (49)$$

According to the D-partition method, the stability region can be determined as the left-hand side of the trajectory in the $f_R(w)$-$f_I(w)$ plane as w increases from zero to infinity. Figure 6 shows three possible shapes of trajectories for various conditions of K_1. Since the value of K_2 is always positive in the actual system, the system becomes stable when the following condition is satisfied:

$$R_0 < K_2 < \infty. \quad (50)$$

3.2.2. Necessary Conditions for the Occurrence of Type-I Instability

In the case of small values of K_1 (i.e., the gravity dominant system), the system becomes asymptotically stable when K_2 is greater than R_0. In other words, the system may encounter the type-I instability region for a certain positive angular frequency when K_2 becomes less than R_0. For larger values of K_1, that is, for the friction dominant system, no solution exists in the positive real axis except for the case of zero angular frequency as shown in Fig. 6-c. In this case the system cannot experience type-I instability because K_2 is always greater than zero in the physical system. From this analysis we can deduce the necessary condition for the occurrence of type-I instability which is corresponding to Fig. 6-a and 6-b. That is,

$$\lim_{w\to 0}\left\{\frac{\partial f_I(w)}{\partial w}\right\}>0 \quad (51)$$

From eq. (49), this inequality reduces to

$$K_1 < 1+\frac{\bar{\tau}_{34}}{\bar{\tau}_{12}}. \quad (52)$$

3.2.3. Conditions for the Occurrence of Flow Excursion

The excursive stability condition for a boiling channel imposing a constant pressure drop can be obtained from the Ledinegg criteria which states that the system is stable if

$$\frac{\partial(\Delta P_{system})}{\partial v}>0 \quad (53)$$

Since the magnitude of the velocity perturbation is an arbitrarily small constant, this criterion can be rewritten as

$$\lim_{s\to 0} Q(s)>0, \quad (54)$$

where Q(s) is the total hydraulic impedance of the system. By applying this criterion to the simplified characteristic equation of the system, we can derive the following condition for the occurrence of excursive instability.

$$K_2 < K_1 - 1. \quad (55)$$

This type of instability may occur for the cases of Fig 6-b and 6-c, especially for very high subcooling conditions.

3.2.4. Characteristics of the Type-I Instability

Assuming a homogeneous flow and low exit quality condition, where $V_{gj}=0$ and $C_r\approx 1$, the

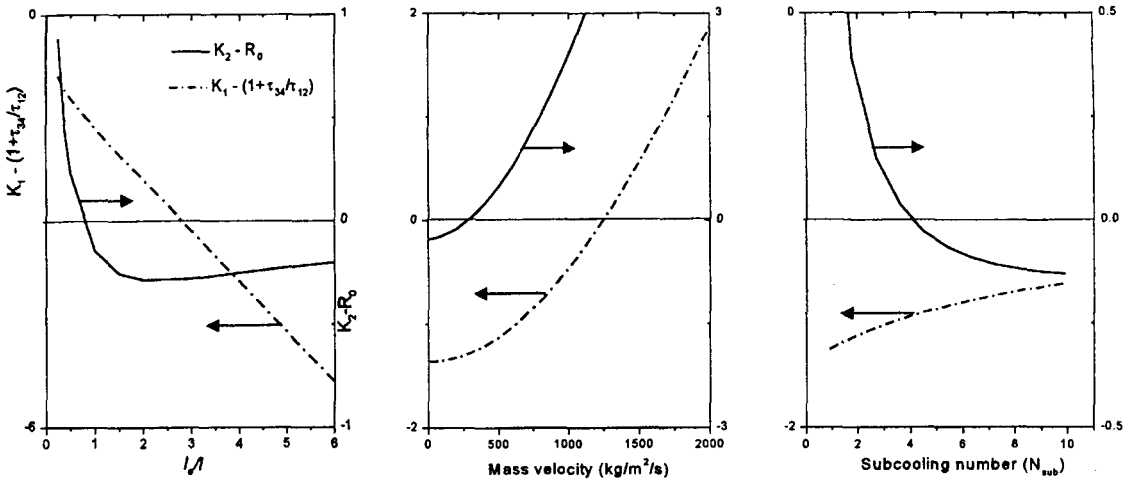

Fig. 7. Parametric Effects on the Type-I Density Wave Oscillation

above inequality, eq. (52), can be approximated as

$$\frac{l_e}{l} > \frac{(F_r + k_e)\cdot N_{fe} - 1}{F_r N_{fe} + 1} \tag{56}$$

This inequality implies that the possibility of occurrence of type-I instability increases as l_e/l increases. In addition, as shown in Fig. 6-c, there exists a threshold value of frictional pressure loss in the unheated riser region beyond which the type-I instability may not occur. Figure 7 shows the parametric effects of the riser length, mass velocity, and subcooling number on the type-I instability. The solid line represents the difference between K_2 and R_0, while the dashed line means the difference of K_1 and its limiting value for the occurrence of type-I instability. Thus, the system becomes unstable when both curves have negative values at the same time. All of these calculations are performed under the constant dimensionless inlet velocity of 0.9. In the case of decreasing mass velocity or increasing subcooling number, the system becomes more unstable in the aspect of type-I instability. In the case of increasing the riser length, the solid line shows a turning point around $l_e/l \approx$. It means that the most dangerous length of the unheated riser for the occurrence of type-I instability may exist for a given boiling channel.

4. Conclusions

Important findings are summarized as follows:

(1) A linear stability analysis model is established by extending Saha' s thermal non-equilibrium model to vertical boiling channels connected with unheated risers. The influence of the two-phase flow models on the analysis of the density wave oscillation is examined. As the result, it reveals that the homogeneous equilibrium model generally under-predicts the heat flux at the onset of the type-II instability. The drift-flux thermal non-equilibrium model employing a flow-regime-dependent drift velocity model, shows good prediction accuracy.

(2) The characteristics of the type-I density wave oscillation are investigated by devising a simplified linear model that takes into account the gravitational and frictional pressure losses.

Simple criteria for the occurrence of the type-I instability and the flow excursion are deduced through the one-dimensional D-partition method. The parametric study reveals that there exists a threshold value of frictional pressure loss in the unheated riser region above which the type-I instability may not occur. Furthermore, it reveals that the most dangerous length of the unheated riser may exist for a given boiling channel.

Acknowledgement

This work was supported by Nuclear R&D Long-Term Development Program of the Ministry of Science and Technology, Republic of Korea.

Nomenclature

A: channel cross-sectional area,
C_0: distribution parameter of void given as eq.(17),
C_l, C_λ: kinematic wave velocity at $z=l$ and $z=\lambda$, respectively,
c_p: specific heat of fluid,
D, D_{hy}: channel diameter, channel hydraulic diameter,
f: friction factor,
F_r: Froude number in the unheated riser region ($=v_{me}^2/gle$),
g: gravitational acceleration,
h: specific enthalpy,
h_{fg}: latent heat of vaporization,
j: volumetric flux density, or $\sqrt{-1}$,
k: form loss factor,
l: length,
N_f: friction number in the heated region ($=f\Phi_m l/2D$),
N_{fe}: friction number in the unheated riser region ($=f_e\Phi_m l_e/2D_e$),
N_{pch}: phase change number ($=\Omega_{eq} l/v_l$),
N_{sub}: subcooling number($=\Omega_{eq}\lambda/v_l$),
P: pressure,
P_e: Peclet number ($=GDc_p/k$)
q'': heat flux,
s: complex variable,
v: velocity,
V_{gj}: drift velocity averaged over the channel cross-sectional area,
V_{gj}^*: non-dimensional drift velocity ($=V_{gj}/v_l$),
α: void fraction,
λ: non-boiling length ($=v\tau_{12}$),
ρ: density,
$\overline{\tau}_{12}$: residence time in the heated single-phase region,
$\overline{\tau}_{34}$: residence time in the unheated riser region,
Φ_m: two-phase pressure drop multiplier,
Γ_g: mass rate of vapor generation per unit volume,
Ω: characteristic frequency of phase change ($=\Gamma_g\Delta\rho/\rho_f\rho_g$),
ξ_h: heated perimeter.

Subscript

e: exit unheated region,
eq: thermal equilibrium state,
f, g: saturated liquid and vapor, respectively,
i: inlet unheated region,
m: two-phase mixture,
λ: at the location of boiling inception.

References

1. H. Mochizuki, "Flow instabilities in boiling channels of pressure-tube-type reactor," *Nuc. Engng. Design*, **149**, 269 (1994).
2. G.C. Park, et al., "The development of a closed form analytical model for the stability analysis of nuclear-coupled density-wave oscillations in boiling water nuclear reactors, *Nuc. Engng. Design*, **92**, 253 (1986).

3. S.J. Peng, et al., "BWR linear stability analysis," Nuc. Engng. Design, 93, 25 (1986).
4. K. Fukuda and T. Kobori, "Classification of two-phase flow instability by density wave oscillation model," *J. Nucl. Sci. Technol.*, **16**, 19 (1979).
5. P. Saha and N. Zuber, "An analytical study of the thermally induced two-phase flow instabilities including the effect of thermal non-equilibrium," *Int. J. Heat Mass Transfer*, **21**, 415 (1978).
6. M. Ishii, *Study on flow instabilities in two-phase mixtures*, ANL-76-23 (1976).
7. D.F. Delmastro, A. Clausse and J. Converti, "The influence of gravity on the stability of boiling flows," *Nuc. Engng. Design*, **127**, 129 (1991).
8. F.S. Wang, L.W. Hu and C. Pan, "Thermal and stability analysis of a two-phase natural circulation loop," *Nuc. Sci. Engng.*, **117**, 33 (1994).
9. D.H. Hwang., Y.J. Yoo and K.K. Kim, *Analysis of two-phase flow instability in vertical boiling channels I: Development of a linear model for the inlet velocity perturbation*, (in Korean) KAERI/TR-1128/98 (1998).
10. N. Zuber and F.W. Staub, "The propagation and the wave form of the vapor volumetric concentration in boiling, forced convection system under oscillatory conditions," *Int. J. Heat Mass Transfer*, 9, 871 (1966).
11. N. Zuber, F.W. Staub, and G. Bijwaard, "Vapor void fraction in subcooled boiling and in saturated boiling systems," *Proc. of 3rd Int. Heat Transfer Conference*, 24 (1966).
12. P. Saha & N. Zuber, "Point of net vapor generation and vapor void fraction in subcooled boiling," *Proc. of 5th Int. Heat Transfer Conference*, **4**, .175 (1974).
13. D.H. Hwang, *Development of a thermal-hydraulic design methodology for an advanced reactor core with vertical parallel channels*, (in Korean) KAERI/TR-992/98 (1998).
14. M. Ishii, *One-dimensional drift-flux model and constitutive equations for relative motion between phases in various two-phase flow regimes*, ANL-77-47 (1977).
15. M.Z. podowski, "Instabilities in boiling systems," *3rd Int. Top. Mtg. NPP Thermal-hydraulics & Operations*, A1-88 (1988).
16. B. Porter, *Stability Criteria for Linear Dynamic Systems*, Chapter 7, Academic Press (1968).
17. K. Ogata, *Modern Control Engineering*, Chapter 9, Prentice-Hall Inc. (1970).
18. D.H. Hwang, Y.J. Yoo, K.K. Kim, M.H. Chang, ALFS: Analysis of Local Flow Stability, Program Reg. Number: 98-01-12-2696, Korea Computer Program Protection Foundation (1998).
19. P. Saha, M. Ishii, and N. Zuber, An experimental investigation of the thermally induced flow oscillations in two-phase systems, *J. Heat Transfer*, **98**, 616 (1976).
20. M.B. Carver, *An analytical model for the prediction of hydrodynamic instability in parallel heated channels*, AECL-2681 (1967).

Appendix

$$\Lambda_{A,f}(s) = 2\rho_f v_i \left(\frac{A}{A_i}\right)^2 \left(\frac{f_i l_i}{2D_i} + k_i\right), \tag{a1}$$

$$\Lambda_{B,f}(s) = \rho_f v_i \frac{f\bar{\lambda}}{2D}\left\{2 + H(s)\right\}, \tag{a2}$$

$$\Lambda_{C,a}(s) = s\rho_f \int_{\bar{\lambda}}^{l}\left(\frac{C_\lambda}{C_z}\right)\Lambda_5(z,s)\,dz, \tag{a3}$$

$$\Lambda_{C,c}(s)=\rho_f v_i\left[C_r^{\,2}v_i\Lambda_4(l,s)+2\left\{\Lambda_5(l,s)-1\right\}+s\int_{\bar{\lambda}}^{l}\left(\frac{C_z}{C_\lambda}\right)\Lambda_4(z,s)dz\right], \tag{a4}$$

$$\Lambda_{C,g}(s)=g\rho_f\left\{\int_{\bar{\lambda}}^{l}\Lambda_4(z,s)dz-\bar{\tau}_{12}H(s)\right\}, \tag{a5}$$

$$\Lambda_{C,f}(s)=\rho_f v_i\frac{f}{2D}\left\{v_i\Phi_m\int_{\bar{\lambda}}^{l}\left(\frac{C_z}{C_\lambda}\right)^2\Lambda_4(z,s)dz+2\Phi_m\int_{\bar{\lambda}}^{l}\Lambda_5(z,s)dz-\bar{\lambda}H(s)\right\}, \tag{a6}$$

$$\Lambda_{C,d}(s)=(1-2C_r)\cdot C_r^{\,2}\rho_g\Lambda_4(l,s)\cdot V_{gj}^{\,2}, \tag{a7}$$

$$\Lambda_{D,a}(s)=\frac{s\rho_f l_e}{C_r}\left(\frac{A}{A_e}\right)\Lambda_5(l,s), \tag{a8}$$

$$\Lambda_{D,g}(s)=g\rho_f l_e R(s)\Lambda_4(l,s), \tag{a9}$$

$$\Lambda_{D,f}(s)=2\rho_f v_i\left(\frac{A}{A_e}\right)^2\left(k_e+\frac{f_e\Phi_m l_e}{2D_e}\right)\Lambda_5(l,s)+\rho_f v_{me}^2\left\{k_e+\frac{f_e\Phi_m l_e}{2D_e}R(s)\right\}\Lambda_4(l,s), \tag{a10}$$

$$\Lambda_{D,d}(s)=\left(e^{-s\bar{\tau}_{34}}-1\right)\Lambda_{C,d}(s), \tag{a11}$$

$$H(s)=\frac{1-e^{-s\bar{\tau}_{12}}}{s\bar{\tau}_{12}}, \tag{a12}$$

$$R(s)=\frac{1-e^{-s\bar{\tau}_{34}}}{s\bar{\tau}_{34}}. \tag{a13}$$